



# Groundwater recharge distribution due to snow cover in shortage conditions (2019–22) on the Gran Sasso carbonate aquifer (Central Italy)

Valeria Lorenzi<sup>1</sup> · Marino Domenico Barberio<sup>2</sup> · Chiara Sbarbati<sup>3</sup> · Marco Petitta<sup>1</sup>

Received: 17 November 2022 / Accepted: 6 April 2023 / Published online: 18 April 2023  
© The Author(s) 2023

## Abstract

Aquifer recharge by the snowpack is relevant to be assessed to evaluate groundwater availability in mountainous karst regions. The recharge due to snowpack in the Gran Sasso aquifer has previously been estimated through an empirical approach using elevation gradients. To validate and quantify the coverage and persistence of the snowpack over time through an objective method, satellite images have been analysed. The Campo Imperatore plain, the endorheic basin acting as a preferential recharge area of the aquifer, plays an important role, both for the snow cover and also for the infiltration and recharge of springs. The identification of recharge areas has been validated by the stable isotope approach with the assessment of computed isotope recharge elevation based on the values and oscillations of the  $\delta^{18}\text{O}$  isotope recorded at the springs. The main findings confirm the high infiltration rate of Campo Imperatore plain and its direct influence on snow contribution to aquifer recharge. The extension of snow coverage out of this plain has a minor influence to recharge, highlighting that the main drivers for infiltration rate are fractured networks and karstic forms more than snow coverage on carbonate outcrops.

**Keywords** Recharge assessment · Karst aquifers · Central Italy · Snow cover · Isotope elevation

## Introduction

Karst aquifers are valuable groundwater resources that provide fresh water to approximately 25% of the human population (Ford and Williams 2007; Chen 2017). They are complex systems of heterogeneous nature and are fundamental in the water supply of European countries and those of the

Mediterranean area, where outcrops of carbonate rocks are very common. In detail, the karst rocks are widespread in the Mediterranean area and constitute 21.6% of the European land surface (Goldscheider et al. 2008). The importance of monitoring available water resources and updating the aquifer recharge is mainly due to the ongoing impact of climate change on these resources and the increase in human abstraction. These two factors are modifying groundwater resource availability. Although groundwater has always shown excellent resilience in adapting to climate change, its careful assessment is required. This is relevant for karst aquifers which are particularly susceptible to climate change impacts (Taylor and Greene 2008). This work aims to validate the amount and the distribution of recharge over the Gran Sasso aquifer for the 2019–2022 period. In detail, the contribution of snowmelt has been investigated, because the rate and timing of snowpack distribution have substantial consequences on aquifer recharge patterns, which in turn affect groundwater availability throughout the year (Earman et al. 2006). Despite its relevance (Colombo et al. 2022), direct measurement and modelling of snowpack effects on aquifer recharge remain challenging due to the inherent limitations of monitoring. Starting from the snow contribution to

---

✉ Marco Petitta  
marco.petitta@uniroma1.it

Valeria Lorenzi  
valeria.lorenzi@uniroma1.it

Marino Domenico Barberio  
marinodomenico.barberio@ingv.it

Chiara Sbarbati  
chiara.sbarbati@unitus.it

<sup>1</sup> Department of Earth Sciences, Sapienza University of Rome, P.Le A. Moro 5, 00185 Rome, Italy

<sup>2</sup> National Institute of Geophysics and Volcanology, Via Di Vigna Murata, 605, 00143 Rome, Italy

<sup>3</sup> Department of Ecological and Biological Sciences, University of Tuscia, Largo Università, 01100 Viterbo, Italy

infiltration calculated by Lorenzi et al. (2022), the obtained results have been compared with Sentinel-2 satellite images for the winter semester (November to April). In this respect, the endorheic basin of Campo Imperatore plain (with an altitude of 1500–1900 m asl) plays a primary role, acting as a preferential zone for infiltration. The plain has therefore been taken into account both for the amount of snow coverage, given its proximity to the highest peaks, but also for being a preferential recharge zone for the aquifer. In fact, many of the main springs may have been fed by not only rainfall but also by snow melt coming from the Campo Imperatore plain (Lorenzi et al. 2022; Scozzafava and Tallini 2001; Amoruso et al. 2014), with an estimation of about 75% of precipitation feeding the aquifer by infiltration. In this scenario, stable water isotopes are useful to understand and delineate the catchment area of the main springs (Barbieri et al. 2005; Sappa et al. 2018; Rusjan et al. 2019; Iacurto et al. 2021). Monitoring changes in stable isotopes over time and space can provide a better understanding of aquifer recharge and spring discharge links, which are critical to the study of groundwater hydrodynamics (Barbieri et al. 2005).

The stable isotopes such as  $\delta^2\text{H}$  and  $\delta^{18}\text{O}$ , acting as conservative tracers (Calligaris et al. 2018; Iacurto et al. 2021), play a key role in the karstic aquifer. In fact, the isotopic concentration of the rainwater impacting the soil is strictly linked to the falling altitude (Giustini et al. 2016). The  $\delta^{18}\text{O}$  and  $\delta^2\text{H}$  stable isotopes have been largely used to determine groundwater recharge areas, with their elevations, and water flow paths (González-Trinidad et al. 2017; Sappa et al. 2018; Wachniew 2015; Arellano et al. 2020; Vespasiano et al. 2015). Applying the use of stable isotopes for calculating the mean recharge elevation is still a basic tool, with particular reference to mountainous aquifers where recharge areas are distributed in a wide elevation range (Petitta et al. 2022). The mean elevation of the recharge area calculated by isotope values of spring water is also representative (Jasechko et al. 2017; Jódar et al. 2021). The major constraint is the knowledge of an average isotopic value of the discharge water, which has been mixed along the flowpath, collecting different inputs from different recharge zones and recharge episodes (Longinelli and Selmo 2003; Minissale and Vaselli 2011; Giustini et al. 2016). Nevertheless, in fractured carbonate aquifers where fast flow in karst conduits is limited, as happens in central Italy, and flow is mainly governed by the fracture network, stable isotopes frequently show steady values with time (Petitta et al. 2015, 2018; Tallini et al. 2014), reducing the seasonal effect of recharge on the groundwater discharge. Within this framework, the aim of the present work is to validate the preliminary assessment of snow on recharge carried out by Lorenzi et al. (2022) through satellite images, as well as to verify through isotopic data how and in which measure spring recharge is influenced by the endorheic basin of Campo Imperatore plain.

## Hydrogeological setting

The Gran Sasso aquifer is defined as a calcareous-karstic system about 1034 km<sup>2</sup> wide and it can be considered one of the most representative karst aquifers of the central-southern Apennines. Its relevance is due to:

- I. The conspicuous amount of water resources deeply exploited for different purposes,
- II. The interaction of human infrastructures with the surface and the groundwater,
- III. The need to provide the enhancement and protection of natural resources in protected areas (National Park) (Adinolfi Falcone et al. 2008).

The Gran Sasso aquifer, characterised by Meso-Cenozoic carbonate units, is bounded by terrigenous units represented by Miocene flysch (regional aquiclude) along its northern side and Quaternary continental deposits (regional aquitard) along its southern side (Amoruso et al. 2014). A single basal regional-wide groundwater table with a hydraulic gradient of 5–20‰ characterizes the flowpath (Tallini et al. 2013; Celico et al. 2005). The Gran Sasso karst aquifer (Fig. 1) feeds springs located at its boundaries, characterised by a total discharge that ranges between 18 and 25 m<sup>3</sup>/s, corresponding to a net infiltration recently recalculated in about 600 mm/y (Lorenzi et al. 2022). Groundwater moves vertically, through the unsaturated zone having a thickness of about 1000 m (Petitta and Tallini 2002). At the massif core, the endorheic basin of Campo Imperatore acts as a preferential recharge area, fed by rainfall and snow melt. This basin, having tectonic-glacial-karstic origins, is 75 km<sup>2</sup> wide and has an elevation that ranges from 1500 to 1900 m asl. The preferential directions of groundwater flow are locally conditioned by the main tectonic discontinuities and are constrained by the altitude of the hydrogeological limits. The discharge includes also a highway tunnel drainage tapped for drinking purposes on both sides. Most of the groundwater is directed towards the sectors where the permeability limits are located at lower altitudes.

The aquifer recharge for the period 2000–2020 was computed in Lorenzi et al. (2022), considering the rainfall, snow and temperature data of four pluviometric gauges (P1–P4 in Fig. 1) and evaluating the gradients by a linear correlation between altitude and precipitation/temperature data. The gradients were then applied from the selected gauges, identifying rainfall and temperature distribution values over the entire aquifer for the 2000–2020 period. In Fig. 2 the monthly rainfall (P1, P2), temperature (P3) and snow (P4) data are shown, while Fig. 3 summarizes the rainfall (A, B) and temperature (C) gradients adopted.

**Fig. 1** Simplified hydro-geological setting of the Gran Sasso aquifer. A Aquitard (continental detrital units of intramontane basins, Quaternary), B aquiclude (terrigenous turbidites, Mio-Pliocene), C aquifer (calcareous sequences, Meso-Cenozoic), D low permeability bedrock (dolomite, upper Triassic), E main thrust, F main extensional fault, P(1–4) selected climatic gauges (P1 and P2 have been considered as reference gauges for rainfall, P3 for temperature and P4 for snow), S(1–14) main springs, G streambed spring, H regional groundwater flow path, I highway tunnel drainage (modified from Tallini et al. 2013)

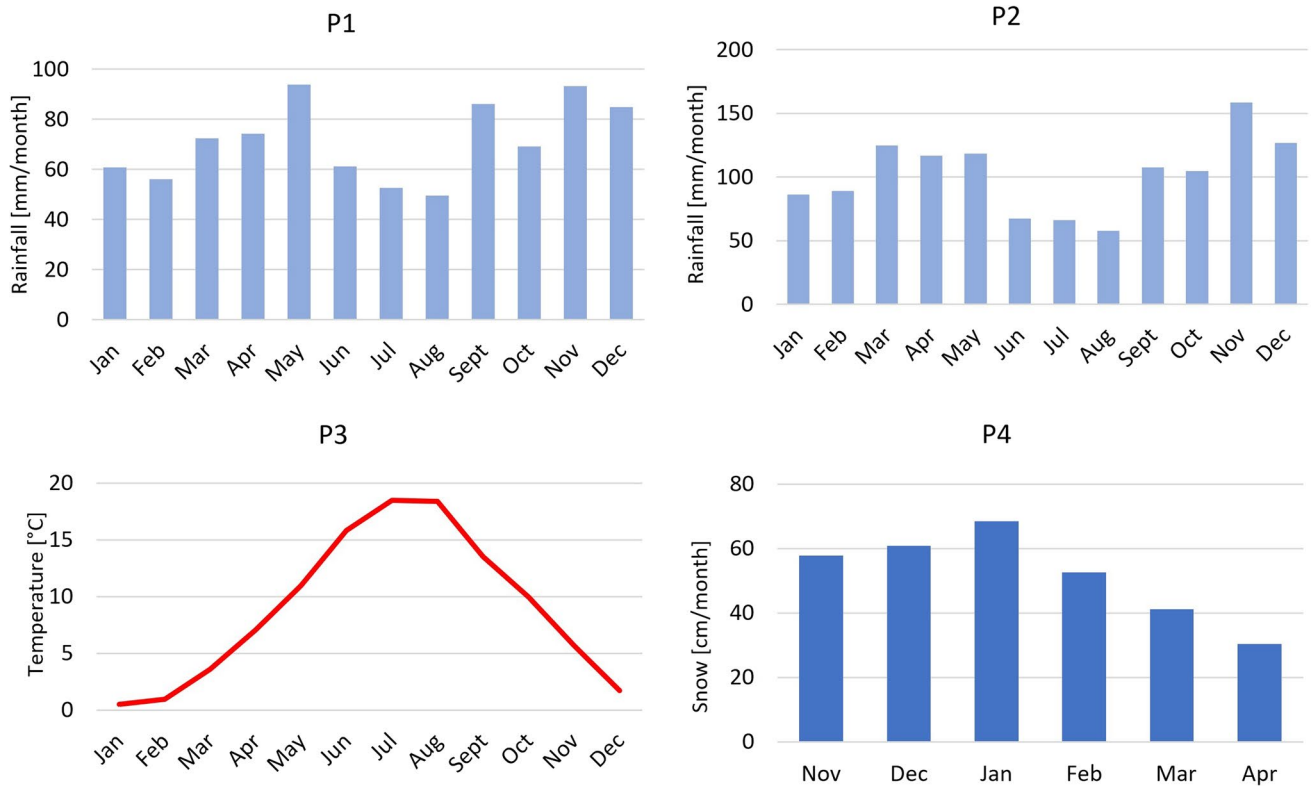
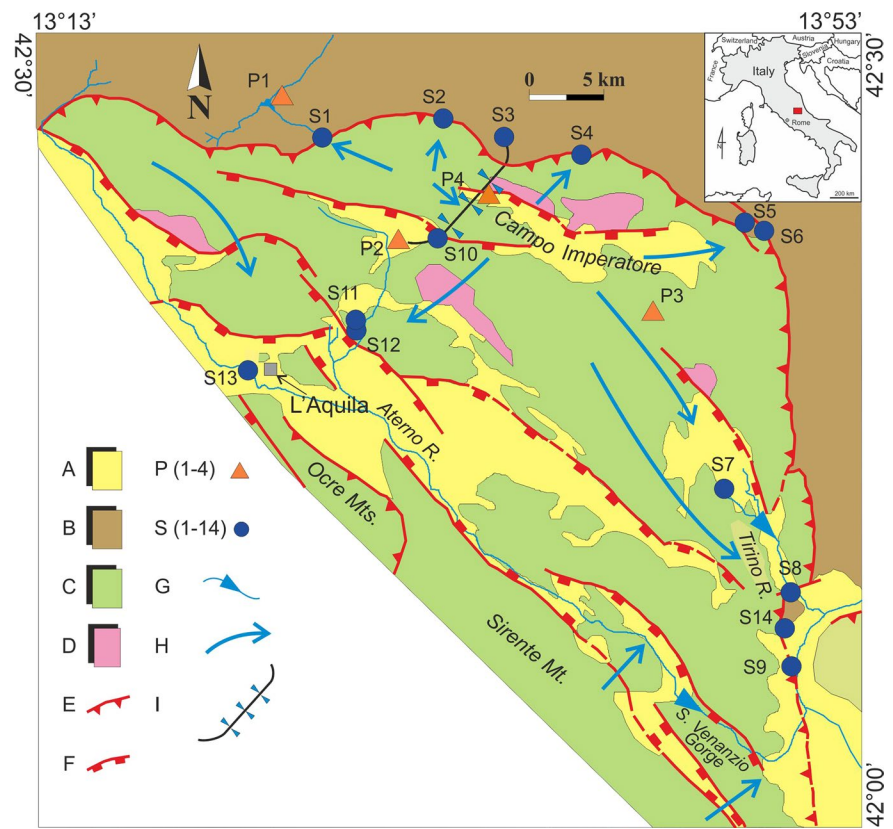


**Fig. 2** Rainfall, temperature and snow monthly data for 2000–2020 period of the four gauges (P1–P4 in Fig. 1), representative of the aquifer recharge. The Campotosto and Assergi gauges (respectively, P1 and P2 in Fig. 1) have been considered as reference data for rain-

fall. The Castel del Monte gauge (P3) has been selected as reference point for temperature. The Campo Imperatore gauge (P4) has been considered for snow coverage

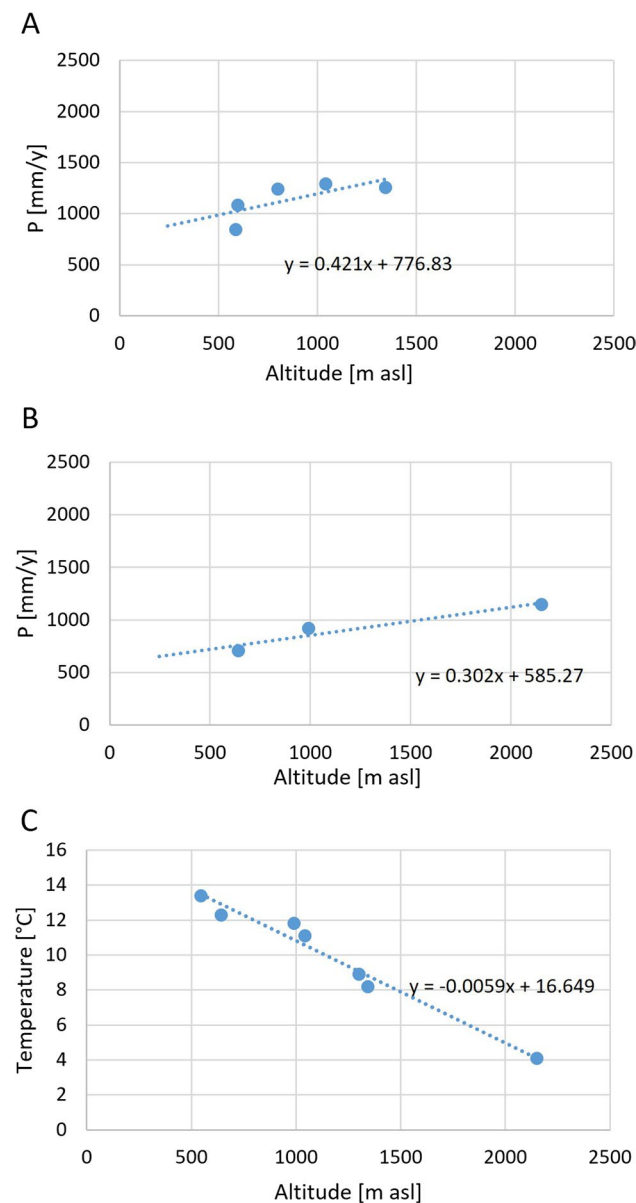


**Fig. 3** The calculated altitude gradients of both rainfall and temperature. The gradients were then applied to identify rainfall distribution values over the entire aquifer for each year (2000–2020). The computed annual rainfall gradients are 42 mm/100 m for the northern slope (A) and 30 mm/100 m for the southern slope (B), while the temperature gradient is  $-0.59$  °C/100 m (C)

The amount of aquifer recharge evaluated in Lorenzi et al. 2022 is 606 mm/y (equivalent to  $16.7$  m<sup>3</sup>/s for the whole aquifer), using the Turc method, 558 mm/y (equivalent to  $15.3$  m<sup>3</sup>/s) using the Thornthwaite method and 594 mm/y (equivalent to  $16.2$  m<sup>3</sup>/s) using the APLIS method (Andreo et al. 2008). The average contribution of snow was estimated in  $3.2$  m<sup>3</sup>/s. The aquifer is characterized by an average effective infiltration rate of 51.6% of total precipitation but an infiltration rate of 76.7% has been assessed by the APLIS

method for the preferential recharge area of the Campo Imperatore basin (Lorenzi et al. 2022). In Fig. 4 the Boxplot of the average monthly rainfall recharge calculated by the Thornthwaite method (A) and the Boxplot of the average monthly snow recharge (B) of the time period considered (2000–2020) are shown.

## Methods

In the study area, the snow melt contribution to recharge appears to be significant (about 20%), and heavily dependent on the snow coverage distribution with space (elevation) and its persistence with time (Lorenzi et al. 2022). The role of high-elevation areas in aquifer recharge becomes even more important considering the influence of snow melting in endorheic basins. The contribution of snow in the 2000–2020 period, calculated by Lorenzi et al. 2022, has been obtained by creating a correlation line between altitude and snow values of the period 1960–1990 (referring to Fazzini and Bisci 1999). The derived monthly gradient for each considered month has been applied to the snow monthly data recorded at the Campo Imperatore gauge (P4 in Fig. 1) to compute the recharge fraction due to snow melt. The snowfall has been converted into equivalent mm of rain (1 cm of snow = 1 mm of rain).

By this way, a snow coverage function of the elevation has been obtained for each month of the winter semester (since November to April), extrapolating a related snow thickness increase with elevation. Since the snow covering and so the snow contribution to the aquifer recharge appears to be strongly related to the elevation, the results of Lorenzi et al. 2022 require a validation, to be obtained through the Sentinel-2 satellite images, offering the real snow coverage of the studied aquifer.

The Gran Sasso aquifer daily images have been downloaded by Esa Sentinel Data Access with a resolution of 10 m (Fig. 5A) and imported into the ArcGis software, where the areas with snow cover have been separated by different colours from those without snow. Images from November 2018 to April 2022 have been examined (Fig. 5B). Some gaps were caused by the lack of useful satellite images but also by satellite images with cloud cover that did not allow for identification of the snow cover limit.

To understand how the preferential infiltration zone (Campo Imperatore plain) can supply the main springs of the aquifer, Computed Isotopic Recharge Elevation (CIRE) has been calculated by the  $\delta^{18}\text{O}$  data. The  $\delta^{18}\text{O}$  values refer to isotopic analyses of samples collected between 2020 and 2022. The monitoring network (Fig. 6) includes 13 main springs and 7 representative monitoring points of the groundwater collected inside the motorway tunnel.

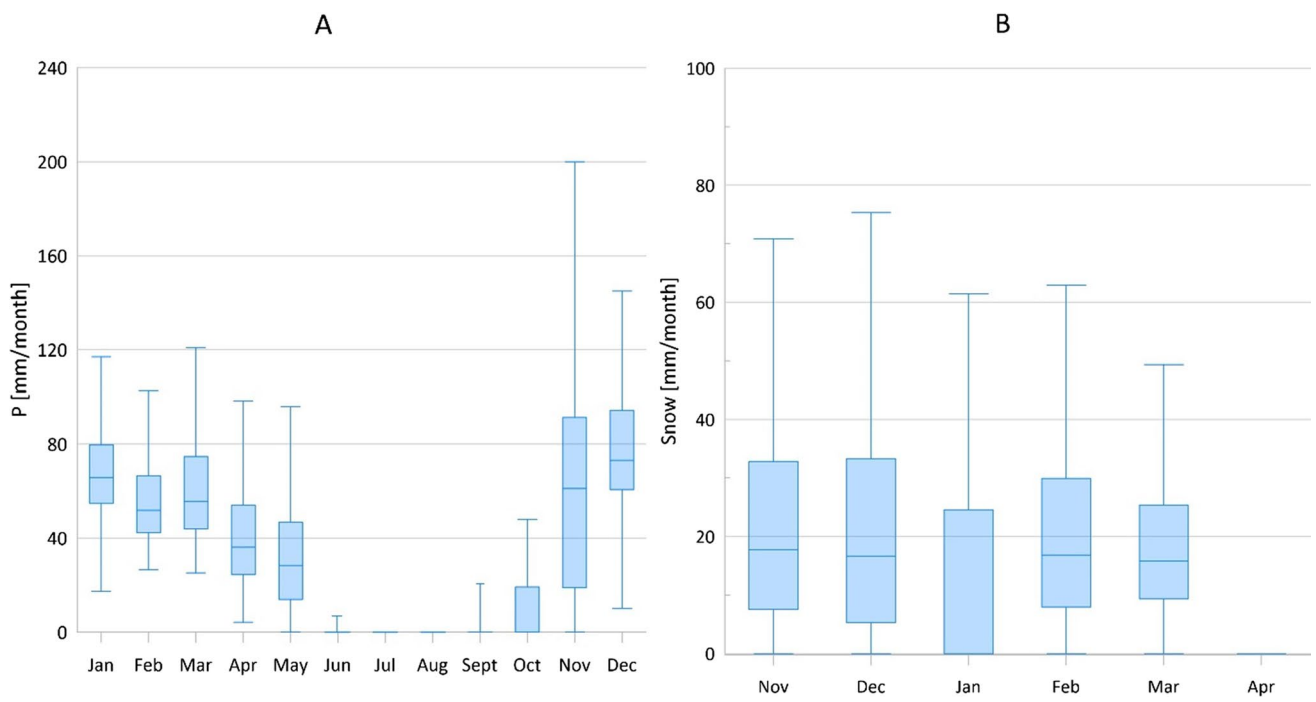


**Fig. 4** **A** Boxplot of the average monthly recharge due to rainfall during the 2000–2020 period calculated by the Thornthwaite method, **B** Boxplot of the average monthly snow recharge during the 2000–2020 period. The whiskers plot indicates the IQR (interquartile range) factor

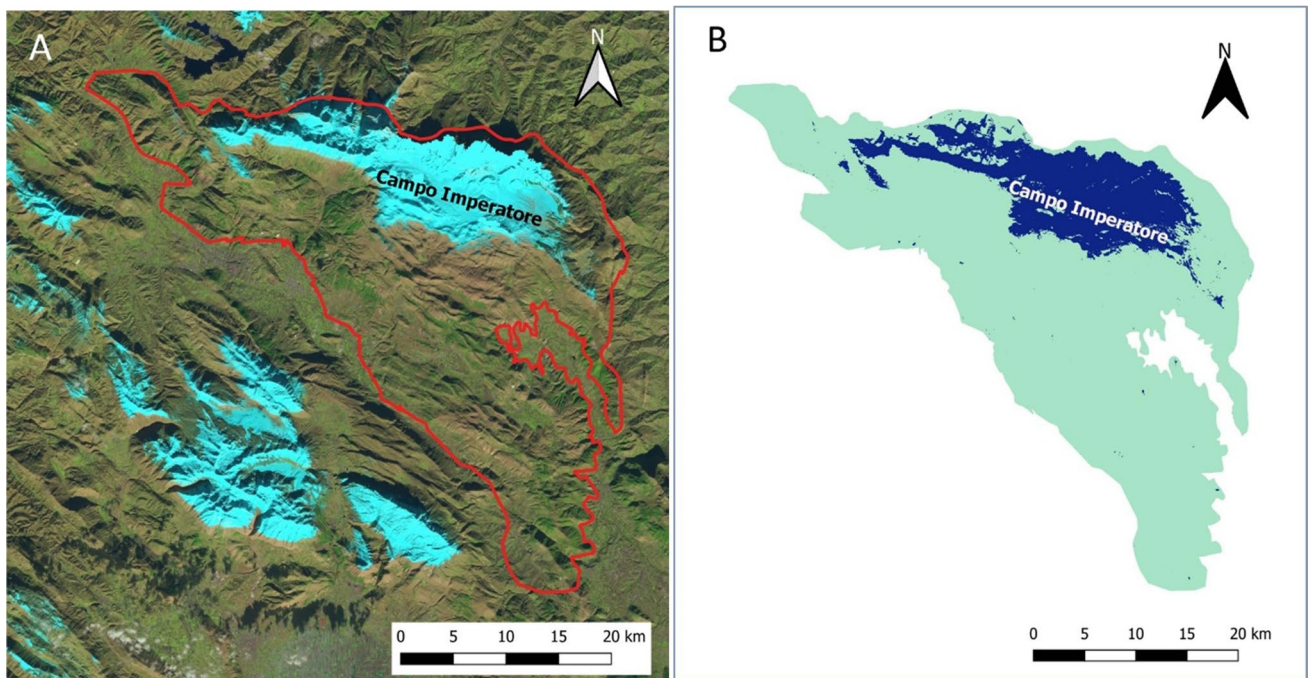
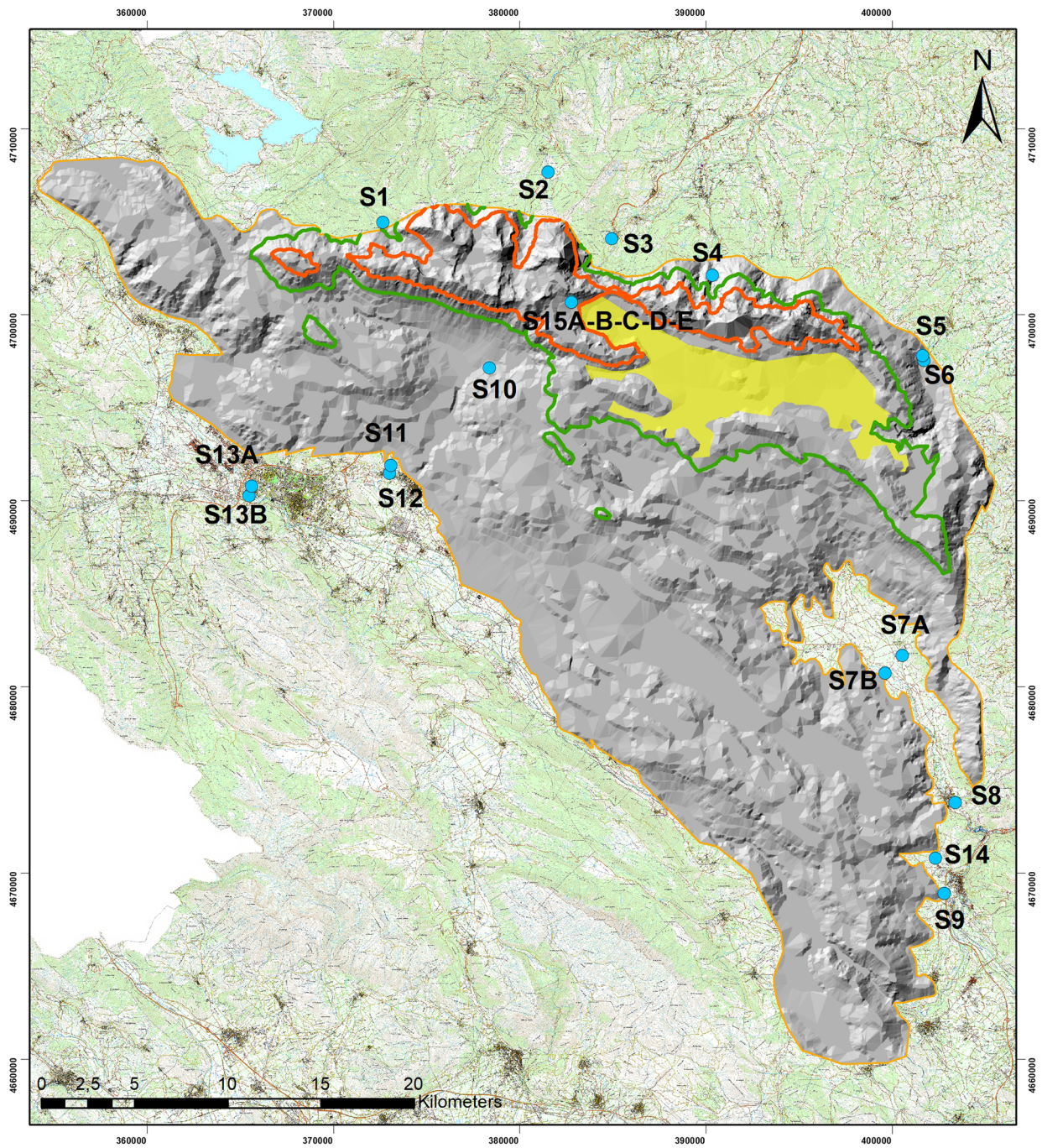


**Fig. 5** **A** Example of an image from ESA Sentinel Data Access with snow coverage in light blue (left panel) related to 18th December 2020, **B** Image elaborated on ArcGis software (right panel) with inferred snow coverage in blue

All the samples have been collected directly from each spring outlet/monitoring points and stored in cool boxes at 4 °C until reaching the isotopes laboratory. Isotopic

composition is expressed in part per mil accordingly to the usual  $\delta$  notation, with respect to the V-SMOW (Vienna Standard Mean Ocean Water). Analysis has been performed



- |                        |                          |                                    |
|------------------------|--------------------------|------------------------------------|
| ● S1-Chiarino          | ● S8- Basso Tirino       | ● S15A-B-C-D-E- Motorway drainages |
| ● S2- Rio Arno         | ● S9-Capo Pescara        | <b>Contour</b>                     |
| ● S3-Northern drainage | ● S10- Southern drainage | — 1500 m asl                       |
| ● S4- Ruzzo            | ● S11- Tempera           | — 1900 m asl                       |
| ● S5- Vitella d'Oro    | ● S12- Vera              | <b>Area</b>                        |
| ● S6- Mortaio d'Angri  | ● S13A- Vetoio           | ■ Campo Imperatore                 |
| ● S7A- Capodacqua      | ● S13B- Boschetto        |                                    |
| ● S7B-Presciano        | ● S14- S.Calisto         |                                    |

**Fig. 6** Location of isotope monitoring points. In red, the 1900 m asl contour and in green 1500 m asl contour have been highlighted. The area of the Campo Imperatore basin is shown in yellow

in the IT2E Isotope Tracer Technologies Europe Srl. Laboratory in Milan (Italy) using a mass spectrometer Finnigan Delta Plus mass equilibrated at 25 °C as described by Epstein and Mayeda (1953) for oxygen. The analytical precision is about  $\pm 0.1\text{‰}$  for  $\delta^{18}\text{O}$  and  $\pm 1\text{‰}$  for  $\delta^2\text{H}$  (Petitta et al. 2022).

Applying the altitude isotope gradient for Gran Sasso aquifer of  $-0.24\text{‰}/100\text{ m}$  (Barbieri et al. 2005) on the isotope values recorded from 2020 to 2022, the CIRE of each spring has been assessed. Specifically, the following equation from Barbieri et al. (2005) has been adopted:  $\delta^{18}\text{O} = -0.0024h - 6.35$ .

## Results and discussion

To evaluate the snow cover extension in  $\text{km}^2$  and the lowest snow elevation, it is helpful to consider the hypsometric curve (Fig. 7).

Table 1 shows the dates of acquisition of the satellite images, the corresponding snow cover area in  $\text{km}^2$  and its lowest elevation for each considered image. Moreover, the lowest snow elevation data calculated by Lorenzi et al. (2022) is reported. Some images have not been accounted for, in particular the 2019–20 winter and data from November of the considered years except 2020. This is due to the absence of images or in some other cases to the low quality due to the presence of clouds.

Obviously, an increase in the extension of snow coverage corresponds with a lower value of the altitude where the snow is detected. It is also worthy of note that November and April are months with limited snow coverage, respect with December, January, February and March.

A comparison of the lowest snow elevations has been carried out between the data derived by Sentinel-2 images and the previous evaluation (Lorenzi et al. 2022). However, the snow cover and also the lowest snow elevation have been based on the days on which satellite images are available, while the previous assessment was made on monthly basis. The results show (Table 1) that the lowest snow elevation calculated by both methods only partially overlaps. An influencing parameter seems to be the extension of the snow cover. This is schematically explained in Fig. 8. The blue line shows the trend of the lowest snow elevation calculated by the gradient (Lorenzi et al. 2022). When the area covered by snow is lower than  $140\text{ km}^2$  the results of the lowest snow elevation previously calculated (Lorenzi et al. 2022) approximately match with the real satellite data (green dots in Fig. 8). For this case, the lowest snow elevation calculated by both methods shows a discrepancy lower than 200 m,

frequently lower than 100 m. Exceeding this threshold, in particular when the snow cover area is between  $140$  and  $220\text{ km}^2$  it has been noted an overestimation of the lowest snow elevation calculated by the use of gradient, with respect to the altitude calculated by satellite images, (grey dotted line in Fig. 8). Only in few cases (when the area covered by snow is wider than  $220\text{ km}^2$ ) the lowest snow elevation calculated with the gradient is underestimated respect with the satellite images (see orange dotted line in Fig. 8).

The two thresholds of the extension of the snow cover correspond to  $140\text{ km}^2$  and  $220\text{ km}^2$  and they can be correlated to the surface area of the Campo Imperatore plain ( $75\text{ km}^2$ ) and its altitude range (1500–1900 m asl). In fact, the threshold of  $140\text{ km}^2$  of snow cover is reached summing the extension of the Campo Imperatore plain ( $75\text{ km}^2$ ) and the outcrops located at an altitude higher than 1900 m asl ( $65\text{ km}^2$ ) on the whole aquifer.

The threshold of  $220\text{ km}^2$  corresponds to the total recharge area of the aquifer located between the altitudes of 2900 m and 1500 m asl, the minimum elevation of the Campo Imperatore plain. Consequently, Campo Imperatore plain and its altitude range have a considerable impact on the snow recharge of the aquifer and the limits of the snow cover. When the snow coverage remains under the threshold of  $140\text{ km}^2$ , only the zones higher than 1900 m asl and part of the Campo Imperatore plain are covered by snow. When the snow coverage enlarges towards  $220\text{ km}^2$ , it includes in addition the areas located at an altitude ranging between 1900 and 1500 m asl out of the Campo Imperatore plain. In the case of snow coverage larger than  $220\text{ km}^2$ , also zones of the aquifer located at lower elevations are covered by snow.

Consequently, monthly gradients have been re-computed to be used when the snow cover area results to be wider than  $140\text{ km}^2$ , splitting the area between  $140$  and  $220\text{ km}^2$  and the area wider than  $220\text{ km}^2$ . When the snow cover area is lower than  $140\text{ km}^2$ , the monthly gradients calculated by Lorenzi et al. (2022) have been used. Data have initially been analysed on a monthly basis. Afterwards, the monthly snow thicknesses (cm) recorded by the Campo Imperatore snow meter gauge on those specific days, its altitude (2139 m asl, slightly above the Campo Imperatore plain) and the lowest snow elevation calculated from real data have been considered to find out updated monthly gradients. During the observation period, the available satellite images corresponding to snow cover area between  $140$  and  $220\text{ km}^2$  are 3 for December, 2 for February and 2 for March, while the satellite images with a snow cover area wider than  $220\text{ km}^2$  are 2 for January and 1 for April. No occurrence of snow coverage  $> 140\text{ km}^2$  has been recorded for November, the starting winter month with limited snowfall.

Through this method, an average snow cover extension and an average lowest snow elevation have been calculated and a new gradient for each considered month has been

**Fig. 7** Hypsometric curve of the considered area. The red line corresponds to the mean elevation value. The points where the altitude values of 1500 m and 1900 m asl intersect the hypsometric curve have been marked with black dots

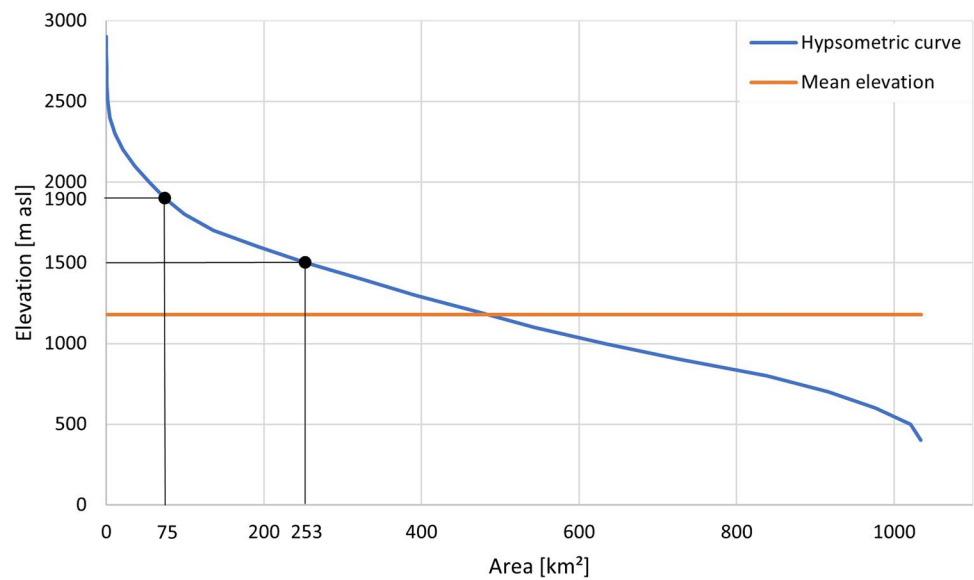


**Table 1** The dates when Sentinel-2 images are available

Date	Snow cover visible	Snow cover extension [km <sup>2</sup> ]	Lowest snow elevation calculated by Lorenzi et al., 2022 [m]	Lowest snow elevation from satellite images [m]
15/11/2018	No			
27/12/2018	Yes	211	300	1475
26/01/2019	Yes	410	1331	970
20/02/2019	Yes	139	1515	1650
22/03/2019	Yes	108	1443	1500
01/04/2019	Yes	94	1315	1550
07/11/2019	No			
15/12/2019	No			
15/01/2020	No			
20/02/2020	Yes	135	1364	1500
15/03/2020	No			
25/04/2020	Yes	29	2150	2100
11/11/2020	Yes	11	2152	2150
16/12/2020	Yes	181	300	1500
15/01/2021	No			
24/02/2021	Yes	190	636	1500
26/03/2021	Yes	204	300	1550
25/04/2021	No			
15/11/2021	No			
31/12/2021	Yes	157	300	1450
15/01/2022	Yes	310	1756	950
09/02/2022	Yes	171	1167	1550
26/03/2022	Yes	160	839	1500
05/04/2022	Yes	227	1713	1300

The presence or absence of cloud cover is also shown. The values of the extent of snow cover and the lowest snow elevation calculated from satellite images and Lorenzi et al. (2022), are included. The lowest snow elevation is highlighted in blue as calculated by Lorenzi et al. (2022). The days when the lowest snow elevations from satellite images match with the lowest snow elevation calculated by gradient (snow cover lower than 140 km<sup>2</sup>) are highlighted in green. The lowest snow elevations that do not match (snow cover between 140 and 220 km<sup>2</sup>) are highlighted in grey. The lowest values of the snow elevation that do not match (snow cover larger than 220 km<sup>2</sup>) are highlighted in orange



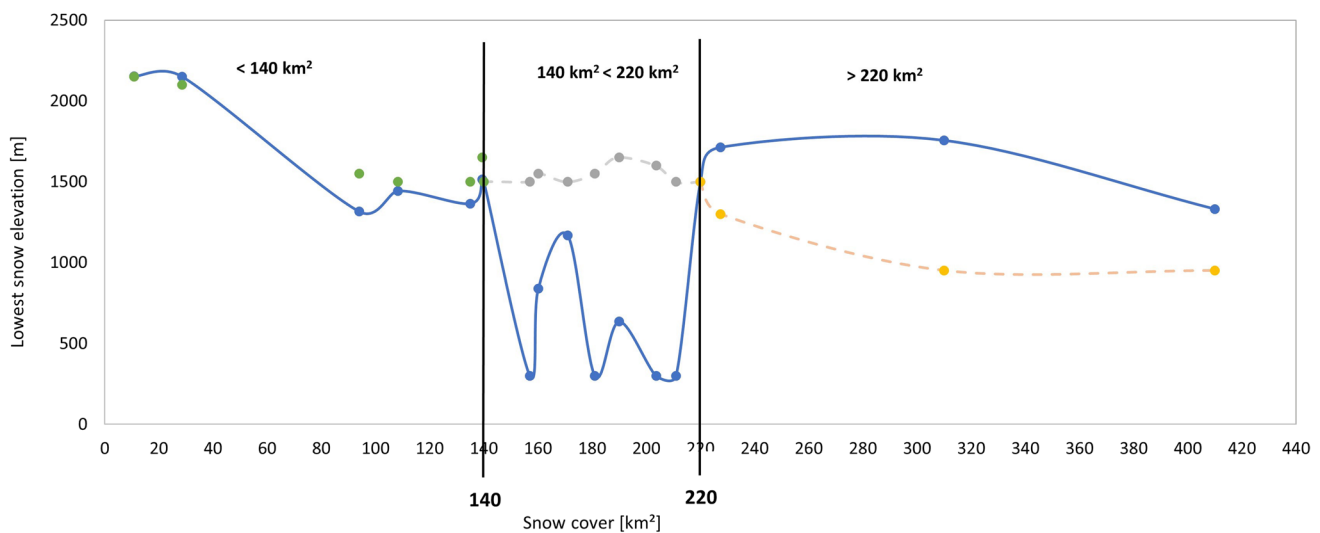


**Fig. 8** Representative scheme of the trend of the lowest snow elevation in relation to snow cover in  $\text{km}^2$  respect with the gradient calculated in Lorenzi et al. (2022) (blue line). In green dots, the lowest snow elevations from satellite images (snow coverage lower than  $140 \text{ km}^2$ ). In grey dotted line, the trend of the lowest snow elevation

evaluated from satellite images adopted to describe the conditions when the snow coverage is between  $140$  and  $220 \text{ km}^2$ . In orange dotted line, the trend of the lowest snow elevation evaluated from satellite images adopted to describe the conditions when the snow coverage is wider than  $220 \text{ km}^2$

computed (Fig. 9). For each considered month, the gradient used by Lorenzi et al. (2022) (in blue dotted line), the newly calculated gradient (in grey or orange dotted line) are shown in Fig. 9. The new applied gradients are:  $10.7 \text{ cm}/100 \text{ m}$  for December,  $6.5 \text{ cm}/100 \text{ m}$  for January,  $10.6 \text{ cm}/100 \text{ m}$  for February,  $9.6 \text{ cm}/100 \text{ m}$  for March and  $3.3 \text{ cm}/100 \text{ m}$  for April. For the lowest snow elevation data of each considered month calculated with the new gradients, see Table 1.

Applying the modified monthly average gradients to the real snow data recorded at the Campo Imperatore snow meter gauge, the contribution of snow to the water recharge has been re-evaluated using the same methodology of Lorenzi et al. 2022, to assess possible changes respect with previous evaluations. In detail, the total recharge in the years 2019 and 2020 results to be negligibly decreased by only  $0.1 \text{ m}^3/\text{s}$ . In this case, for the whole aquifer the snow coverage seems not to have a significant influence on aquifer recharge: in fact, snow coverage does not extend over  $140 \text{ km}^2$ , except in one case (Table 1). Conversely, 2021 and 2022 are characterised by persistent snow cover wider than  $140 \text{ km}^2$  within considered months and therefore the snow recharge values have been re-calculated. As a result, 2021 is characterised by a lower snow recharge respect with to previous estimations with a shortage of  $2.2 \text{ m}^3/\text{s}$  (from  $3.4$  to  $1.2 \text{ m}^3/\text{s}$ ), while 2022 is characterised by a lowering of  $2 \text{ m}^3/\text{s}$  (from  $3.5 \text{ m}^3/\text{s}$  to the value of only  $1.5 \text{ m}^3/\text{s}$  calculated by satellite images). From these results, it can be assessed that the contribution of snowfall to aquifer recharge has a relevant role mainly inside Campo Imperatore plain (snow coverage  $< 140 \text{ km}^2$  and larger but at higher altitudes), while the snowfall

exceeding this area at lower elevations ( $> 220 \text{ km}^2$ ) has a limited impact on aquifer recharge, to be reevaluated as lower than previously calculated. This finding reinforces the role of fracture networks and karst features in aquifer recharge, limiting the impact of slopes and rock outcrop areas at least for snow recharge. Taking into account the key role of the Campo Imperatore plain on the aquifer recharge due to snow cover, stable isotope data from springs have been used to verify how much spring discharge is affected by preferential infiltration from Campo Imperatore. In Table 2, the stable isotope results of  $\delta^{18}\text{O}$  of springs sampled in 2020–2022 and the CIRE calculated by equation from Barbieri et al. (2005) are listed. In Fig. 10 the data from Table 2 are reported. In particular, the figure shows the CIRE values (green, blue and red dots) calculated by an equation from Barbieri et al. (2005) (black line).

Box plots in Fig. 11 resume the CIRE elevation of each spring of the Gran Sasso aquifer, considering the isotopic data since 2020–2022. The red dotted lines indicate the altitude range of the Campo Imperatore plain ( $1500$ – $1900 \text{ m asl}$ ), while the whiskers plot indicates the IQR (interquartile range) factor.

The springs located on the northern slope (S1–S2–S4–S5–S6, Fig. 1) show similar and steady values of  $\delta^{18}\text{O}$  (average  $-10.5\text{‰}$ ) and are characterised by a CIRE ranging from  $1600$  to  $1900 \text{ m asl}$ , clearly corresponding to recharge coming from the same elevations of Campo Imperatore endorheic basin. Consequently, it can be inferred that these springs can receive a significant contribution from the Campo Imperatore recharge area.

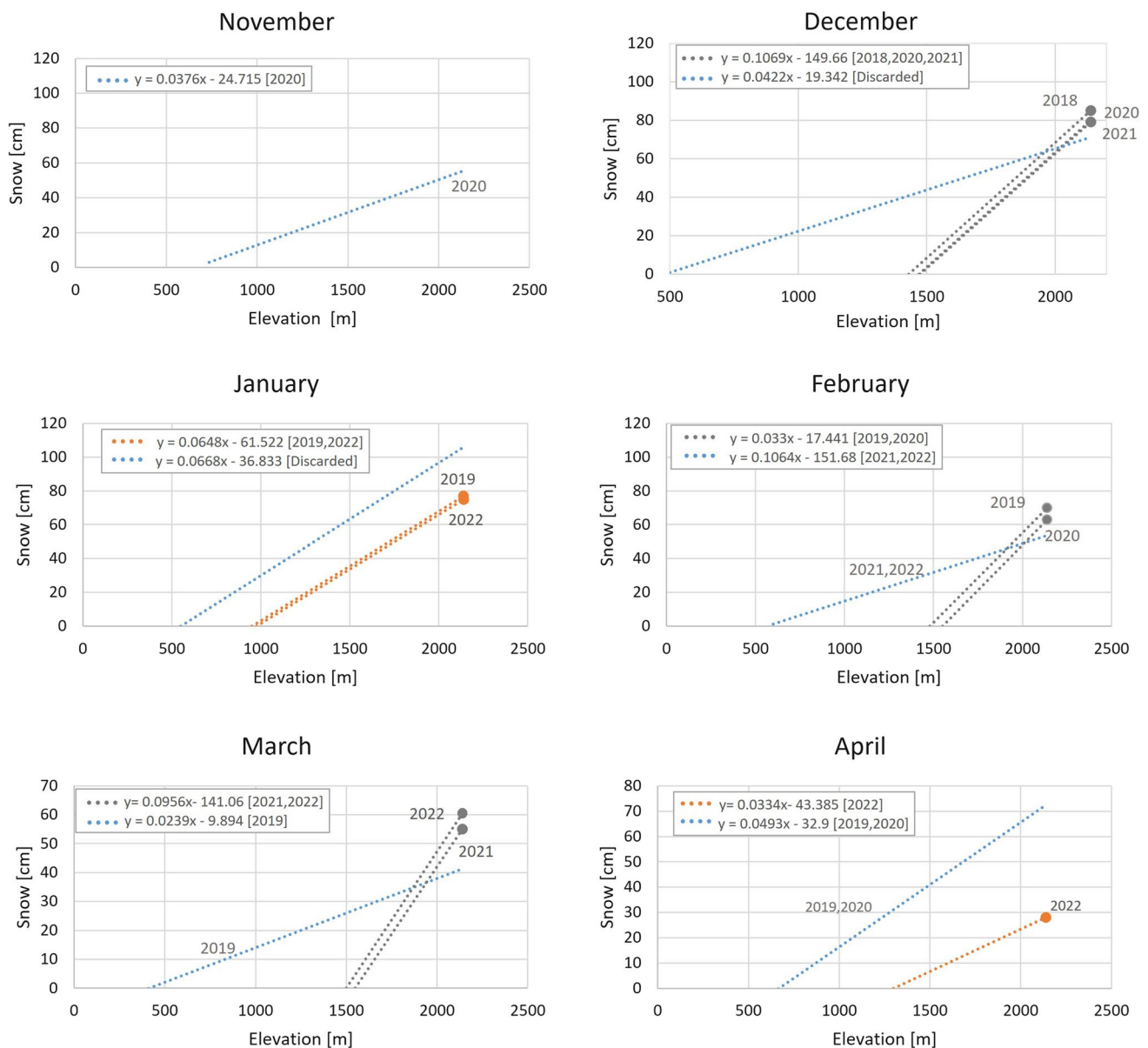


**Fig. 9** New monthly gradients adopted to assess the real snow cover extension. In blue: the monthly gradient calculated by Lorenzi et al. (2022). In grey, the new monthly gradient obtained from Sentinel-2 images when the snow cover area is between 140 and 220 km<sup>2</sup>. In

orange the new monthly gradient obtained from Sentinel-2 images when the snow cover area is wider than 220 km<sup>2</sup>. The graphs specified the years when the gradient has been used. The dots indicate the real values measured in P4 (see Fig. 1 for location)

The sole spring on the northern side characterised by an isotopic recharge elevation having larger variability is the Ruzzo spring (S4), ranging from 1546 to 1850 m asl. This anomaly can be linked to the high variability of the spring's flow rate, characterised by flow having some runoff component and rapid circuits (Petaccia and Rusi 2008). Anyway, its larger variability remains included in the recharge altitude range of the Campo Imperatore plain.

The springs located in the southeastern area (S7A, S7B, S9, S14) also appear to be at least partially fed by water from the Campo Imperatore plain, showing lower CIRE respect

with the northern ones, but their values are still at the lower boundary of the Campo Imperatore altitude. These springs represent the ultimate drainage of the regional water table, with considerable and constant flow rates over time. Moreover, S9, Capo Pescara spring, is characterised by a different origin of the recharge, coming from both the two aquifers of Gran Sasso and Sirente mountains (Lorenzi et al. 2022; Scozzafava and Tallini 2001; Petitta and Tallini 2002).

The springs on the L'Aquila side, although located at the same altitude (650 m asl), show different values of CIRE: S11 and S12 are characterised by a CIRE between 1700

**Table 2** Isotopic values of  $\delta^{18}\text{O}$  of the main springs of the aquifer and the IE (Isotopic Elevation) calculated by using the CIRE equation (Computed Isotopes Recharge Elevation) from Barbieri et al., 2005

ID	2020		2021		2022		2020		2021		2022				
	$\delta^{18}\text{O}$	IE	$\delta^{18}\text{O}$	IE	$\delta^{18}\text{O}$	IE	$\delta^{18}\text{O}$	IE	$\Delta^{18}\text{O}$	IE	$\delta^{18}\text{O}$	IE			
S1	- 10.8	1850	- 10.1	1546	- 10.4	1671	S9		- 10.1	1546					
			- 10.4	1671					S10	- 11.0			1939	- 11.1	1982
			- 10.4	1671						- 11.4			2113		
			- 10.7	1792					S11	- 11.0			1939	- 10.6	1776
S2	- 10.6	1776	- 10.2	1608	- 10.3	1626			- 10.8	1850	- 10.7	1792			
			- 10.3	1626			- 10.6	1776							
			- 10.6	1776			- 11.0	1939							
			- 10.7	1792			S12	- 10.6	1776	- 10.6	1776	- 10.6	1776		
S3	- 11.3	2072	- 10.8	1850	- 10.8	1850			- 10.7	1792	- 10.6	1776			
			- 11.1	1982			- 10.9	1901	- 10.8	1850					
			- 10.3	1626			- 11.0	1939							
			- 9.7	1384			S13A	- 9.1	1159	- 9.2	1185	- 9.2	1185		
S4	- 10.1	1546	- 10.3	1626					- 9.3	1223	- 8.9	1062			
			- 10.8	1850	- 10.3	1626									
S5	- 10.7	1792	- 10.2	1608	- 10.2	1608			- 9.6	1346					
			- 10.2	1608			- 10.3	1626	S13B	- 9.6	1346	- 9.4	1285	- 9.3	1223
			- 10.5	1725			- 10.5	1725	- 9.3	1223	- 9.4	1285			
			- 10.6	1776			- 10.6	1776	- 10.5	1725					
S6	- 10.8	1850	- 10.5	1725	- 10.5	1725	S14		- 9.7	1384					
			- 10.5	1725					- 10.5	1725	- 9.7	1384			
			- 10.6	1776					- 10.7	1792					
			- 10.8	1850					S15A	- 11.2	2017	- 11.7	2215		
S7A	- 10.4	1671	- 10.2	1608			S15B	- 11.2	2017	- 11.3	2072				
			- 10.3	1626	- 11.5	2162									
			- 10.4	1671	S15C	- 11.1	1982	- 11.2	2017						
			- 10.6	1776	- 11.3	2072									
S7B	- 10.2	1608	- 9.9	1460			S15D	- 11.1	1982	- 11.2	2017				
			- 10.0	1509	- 11.4	2108									
			- 10.5	1725	S15E	- 11.0	1939	- 11.0	1939						
			- 10.2	1608	- 11.4	2108									

ID refers to Fig. 3

and 1900 m asl, while S13A and S13B are characterised by a lower isotopic elevation, between 1100 and 1300 m asl. From these data can be inferred that the recharge of S11 and S12 can be attributed to the Campo Imperatore basin too, considering they have evidence of fast-circulating groundwater directly connected to the aquifer core (Petitta and Tallini 2002). The S13A and S13B springs, on the other hand, are probably fed by recharge coming from the carbonate ridges having lower elevation, with the possible influence of the deposits of the L'Aquila plain (Petitta and Tallini 2002), resulting in a lower CIRE.

The monitoring points inside the motorway tunnel (S3, S10, S15A-E) are the most depleted in  $\delta^{18}\text{O}$  of the entire Gran Sasso aquifer (average  $\delta^{18}\text{O} = - 11.1 \text{ ‰}$ ) and consequently they have a very high isotopic recharge elevation, mainly above 2000 m. The S3 monitoring point is the

only one showing large isotopic value variability, ranging from  $\delta^{18}\text{O}$  value of  $- 9.7 \text{ ‰}$  (corresponds to CIRE value of 1384 m asl) to  $- 11.3 \text{ ‰}$  (corresponds to CIRE value of 2072 m asl). On the basis of local hydrogeological and hydrochemical settings (Barbieri et al. 2005; Petitta and Tallini 2002; Tallini et al. 2013), the CIRE results suggest that groundwater directly crosses the unsaturated zone (approximately 1000 m thick), reaching highway tunnels (aquifer core) coming prevalently from the elevations higher than Campo Imperatore plain. The possibility of a secondary contribution from the preferential recharge zone of the aquifer cannot be excluded.

To sum up, most of the CIRE attributed to the main springs of the Gran Sasso aquifer are compatible with the significant recharge contribution from Campo Imperatore basin, confirming its primary role in the aquifer recharge,

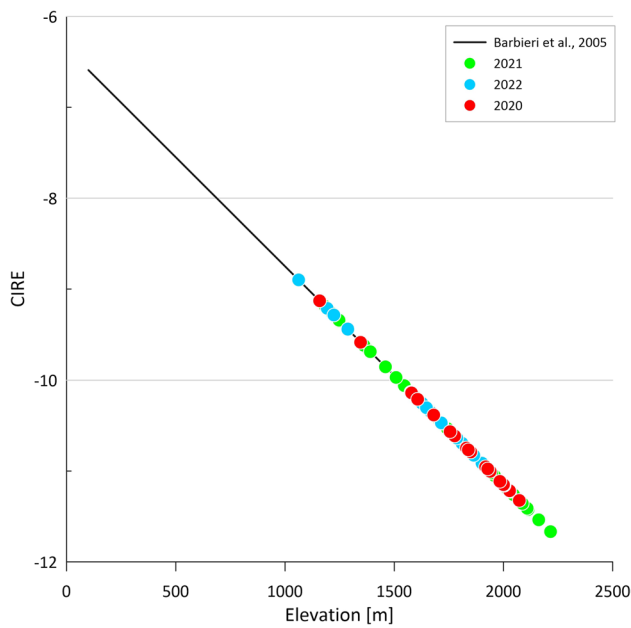


**Fig. 10** Correlation between elevation and CIRE values calculated for the 2020–2022 period based on the CIRE equation from Barbieri et al. (2005) (black line)

supporting the previous estimation in over 75% of precipitation values feeding infiltration from this endorheic basin.

Figure 12 shows a conceptual hydrogeological scheme summarising the results of updated snow recharge evaluations and isotopic recharge values. The hydrogeological section is carried out in the NE–SW direction, connecting the S3 and S11 springs. The figure summarises the aim of the work, from the assessment of snow quantity and its distribution to the verification through isotopic data of how the contribution of snow recharge can influence the springs located at the aquifer boundaries.

### Conclusion

Snow cover contribution to the water budget in mountainous karst areas is frequently significant for aquifer recharge, but the relationships with its extension and karst preferential infiltration zones is still not clear. By considering the snow cover through satellite images over the period 2019–2022, it has been observed that the snow cover extension does not always coincide with its calculation based on altitude

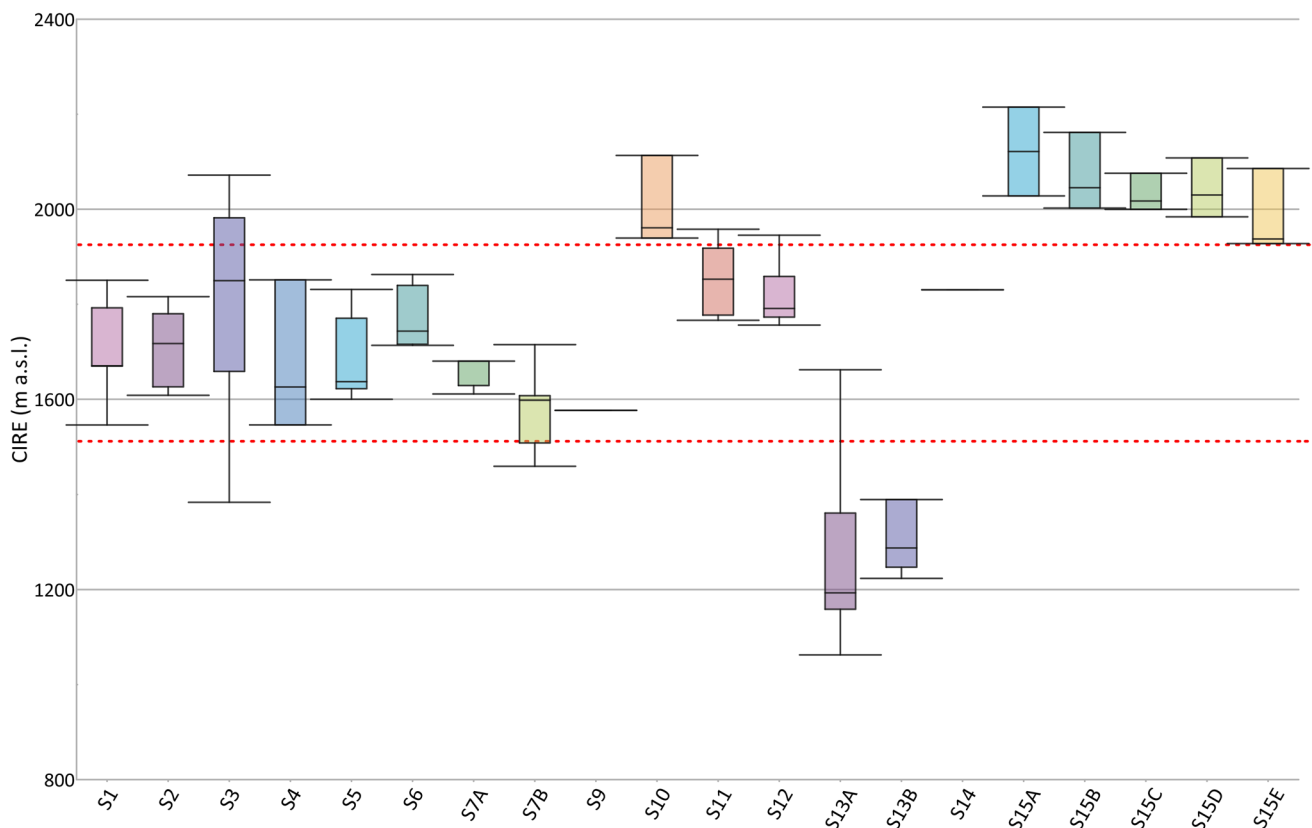


**Fig. 11** Box plot of the CIRE elevation of each isotope monitoring point of the Gran Sasso aquifer. Red dotted lines indicate the altitude range of Campo Imperatore plain (1500–1900 m asl). The whiskers plot indicates the IQR factor (interquartile range). Spring ID refers to Fig. 6

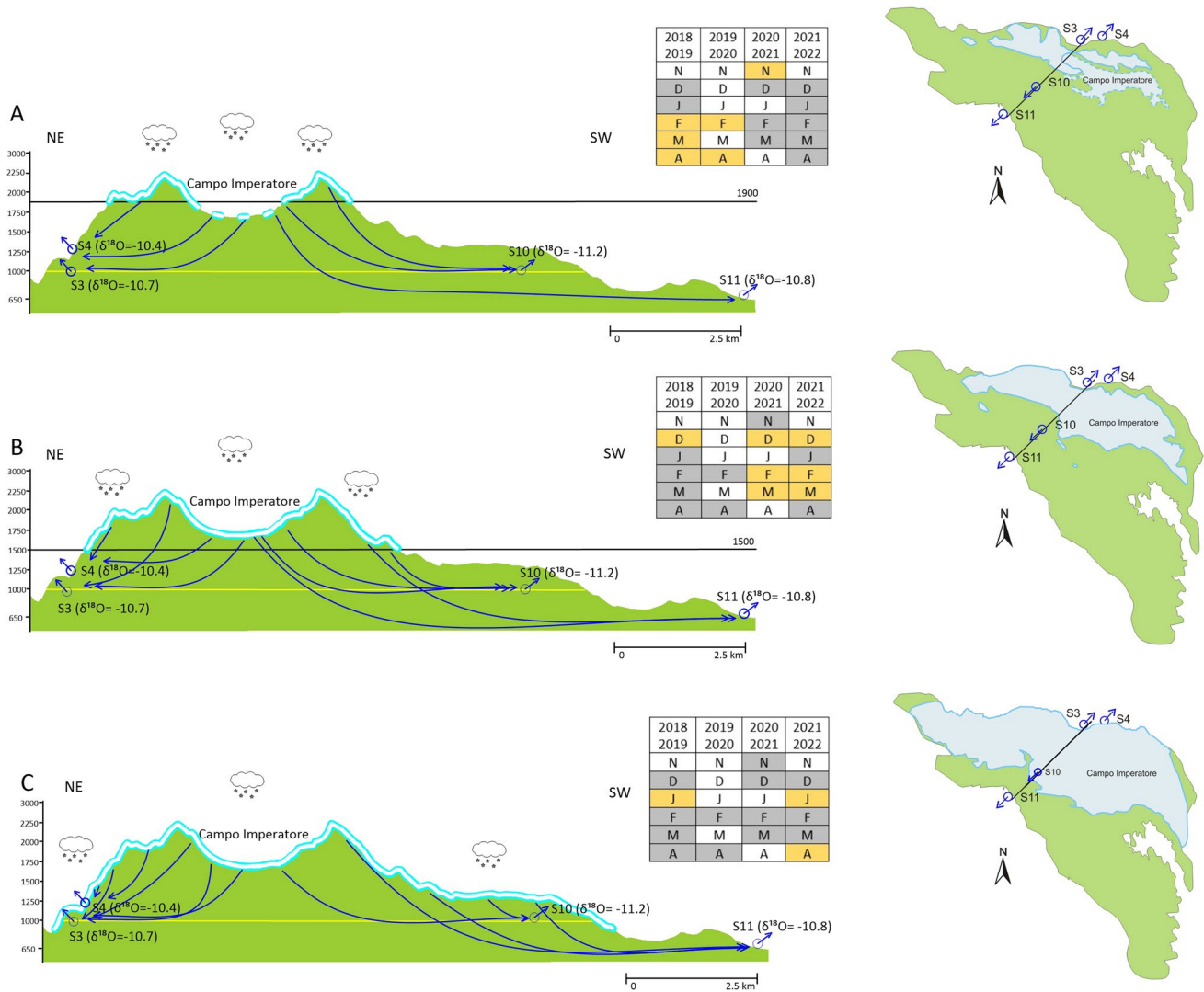


**Fig. 12** Hydrogeological scheme of the three different scenarios of the snow coverage in relation to the lowest snow elevation. The highway tunnel is shown in yellow. The lines with arrows indicate the snow recharge contribution to groundwater flow, according to the isotope evaluation. The average  $\delta^{18}O$  values of the S3, S4, S10 and S11 springs are included. **a** When the snow coverage is under the threshold of 140 km<sup>2</sup>, only the zones higher than 1900 m asl and part of the Campo Imperatore plain are covered by snow. **b** When the snow coverage is between 140 and 220 km<sup>2</sup>, it includes in addition the areas

located at an altitude ranging between 1900 and 1500 m asl out of the Campo Imperatore plain. **c** In case of snow coverage larger than 220 km<sup>2</sup>, also zones of the aquifer located at lower elevations are covered by the snow. On the right, the corresponding maps of the aquifer with the related snow coverage extension (in light blue) are shown. The small tables highlight in yellow the months in the studied period corresponding to a, b or c conditions. In grey, the months with satellite images available for evaluation; in white months without valid satellite images

gradient data (Lorenzi et al. 2022). In detail, a strong correspondence between the snow cover extension on Campo Imperatore plain and snow recharge contribution has been reinforced by the comparison with satellite images.

Based on the recorded data, new monthly gradients have been calculated, to be applied during months when the snow cover is larger than 140 km<sup>2</sup> and specially when it is larger than 220 km<sup>2</sup>, involving areas out of the main recharge plain, at lower elevations. Results for 2019–22 confirmed the significant role of the aquifer recharge

by the snow covering Campo Imperatore plain. In fact, recharge from snow in 2019–20, when the snow coverage did not exceed the plain boundaries, has been confirmed in about 15% of the total aquifer recharge, as previously assessed. Conversely, in both winter semesters of 2021–22, the snow coverage frequently exceeded the plain limits, but the recalculated recharge shows how the infiltration from snow located out of Campo Imperatore is very limited, leading to an updated evaluation of snow recharge lower than the one previously assessed (up to

– 60%). This finding reinforces the role of karst features in aquifer recharge from snow, possibly driven by snow melt, and consequently it limits the significance of wide snow coverage periods to the infiltration process.

The stable isotope data collected in this study have been used to validate the significant role of Campo Imperatore in the aquifer recharge. In particular, it has been observed how the CIRE of the main springs frequently confirmed a recharge directly coming from the Campo Imperatore plain. This finding confirmed, at least for fractured carbonate aquifers, that the distribution of recharge is correlated with altitude and karst landscape occurrence. The Campo Imperatore plain, specifically in this case, is therefore the fundamental site to calculate the snow cover and in particular its contribution to aquifer recharge. In future scenarios influenced by climate change effects, the accurate knowledge of recharge due to snow cover, both in terms of preferential infiltration areas and extension, is a primary goal for ensuring a reliable renewable water resource evaluation.

**Acknowledgements** The authors would like to thank IT2E Isotope Tracer Technologies Europe Srl. Laboratory in Milan (Italy) for providing the isotopic composition analyses. Thanks go to all members of the Quantitative Hydrogeology Lab, Earth Sciences Department, Sapienza University of Rome for their logistic and technical support. Thanks go to the Water Utilities ACA, Ruzzo Reti and Gran Sasso Acqua for allowing access to tapped spring for samplings. The logistic support of the Commissioner for the Gran Sasso Hydraulic Emergency, especially for highway tunnel surveys, was warmly appreciated. Discussions with the KARMA project partners during remote meetings, and consequent suggestions, were also highly appreciated.

**Author contributions** VL: conceptualization, methodology, investigation, data curation, writing—original draft. MDB: methodology, writing—review and editing. CS: data curation, writing—review and editing. MP: conceptualization, methodology, writing—review and editing, supervision, project administration.

**Funding** Open access funding provided by Università degli Studi di Roma La Sapienza within the CRUI-CARE Agreement. The research has been supported by the European Commission through the Partnership for Research and Innovation in the Mediterranean Area (PRIMA) programme under Horizon 2020 (KARMA project, grant agreement number 01DH19022A).

**Data availability** The datasets used and/or analyzed during the current study are available from the corresponding author on reasonable request. Additionally, all data used in this study are included in the official deliverables of KARMA EU project, available at <http://karma-project.org/>.

## Declarations

**Conflict of interest** The authors declare that they have no known competing financial interests or personal relationships that could have appeared to influence the work reported in this paper.

**Open Access** This article is licensed under a Creative Commons Attribution 4.0 International License, which permits use, sharing, adaptation, distribution and reproduction in any medium or format, as long as you give appropriate credit to the original author(s) and the source, provide a link to the Creative Commons licence, and indicate if changes

were made. The images or other third party material in this article are included in the article's Creative Commons licence, unless indicated otherwise in a credit line to the material. If material is not included in the article's Creative Commons licence and your intended use is not permitted by statutory regulation or exceeds the permitted use, you will need to obtain permission directly from the copyright holder. To view a copy of this licence, visit <http://creativecommons.org/licenses/by/4.0/>.

## References

- Adinolfi Falcone R, Falgiani A, Parisse B, Petitta M, Spizzico M, Tallini M (2008) Chemical and isotopic ( $\delta^{18}\text{O}_{\text{cc}}$ ,  $\delta^2\text{H}_{\text{cc}}$ ,  $\delta^{13}\text{C}_{\text{cc}}$ ,  $^{222}\text{Rn}$ ) multi-tracing for groundwater conceptual model of carbonate aquifer (Gran Sasso INFN underground laboratory—central Italy). *J Hydrol* 357:368–388. <https://doi.org/10.1016/j.jhydrol.2008.05.016>
- Amoruso A, Crescentini L, Petitta M, Rusi S, Tallini M (2011) Impact of the 6 April 2009 L'Aquila earthquake on groundwater flow in the Gran Sasso carbonate aquifer, Central Italy. *Hydrol Process* 25:1754–1764. <https://doi.org/10.1002/hyp.7933>
- Amoruso A, Crescentini L, Martino S, Petitta M, Tallini M (2014) Correlation between groundwater flow and deformation in the fractured carbonate Gran Sasso aquifer (INFN underground laboratories, central Italy). *Water Resour Res* 50:4858–4876. <https://doi.org/10.1002/2013WR014491>
- Andreo B, Vias J, Duran J, Jimenez P, Lopez-Geta JA, Carrasco F (2008) Methodology for groundwater recharge assessment in carbonate aquifers: application to pilot sites in southern Spain. *Hydrogeol J* 16:911–925. <https://doi.org/10.1007/s10040-008-0274-5>
- Arellano LN, Good SP, Sánchez-Murillo R, Jarvis WT, Noone DC, Finkenzler CE (2020) Bayesian estimates of the mean recharge elevations of water sources in the Central America region using stable water isotopes. *J Hydrol Reg Stud* 32:100739. <https://doi.org/10.1016/j.ejrh.2020.100739>
- Barbieri M, Boschetti T, Petitta M, Tallini M (2005) Stable isotope ( $^2\text{H}$ ,  $^{18}\text{O}$  and  $^{87}\text{Sr}/^{86}\text{Sr}$ ) and hydrochemistry monitoring for groundwater hydrodynamics analysis in a karst aquifer (Gran Sasso, Central Italy). *Appl Geochem* 20:2063–2081. <https://doi.org/10.1016/j.apgeochem.2005.07.008>
- Calligaris C, Mezga K, Slejko FF, Urbanc J, Zini L (2018) Groundwater Characterization by Means of Conservative ( $\delta^{18}\text{O}$  and  $\delta^2\text{H}$ ) and Non-Conservative ( $^{87}\text{Sr}/^{86}\text{Sr}$ ) Isotopic Values: The Classical Karst Region Aquifer Case (Italy–Slovenia). *Geosciences* 8(9):321. <https://doi.org/10.3390/geosciences8090321>
- Celico P, Fabbrocino S, Petitta M, Tallini M (2005) Hydrogeological impact of the Gran Sasso motor-way tunnels (Central Italy). *G Di Geol Appl* 1:157–165. <https://doi.org/10.1474/GGA.2005-01-0-16.0016>
- Chen Z (2017) Modeling a geologically complex karst aquifer system, Hochifen-Gottesacker. *Alps. KIT-Fak. fü BGU* 1–111
- Coleman ML, Shepherd TJ, Durham JJ, Rouse JE, Moore GR (1982) Reduction of water with zinc for hydrogen isotope analysis. *Anal Chem* 54(6):993–995. <https://doi.org/10.1021/ac00243a035>
- Colombo N, Valt M, Romano E, Salerno F, Godone D, Cianfarra P, Freppaz M, Maugeri M, Guyennon N (2022) Long-term trend of snow water equivalent in the Italian Alps. *J Hydrol*. <https://doi.org/10.1016/j.jhydrol.2022.128532>
- Di Celso GM, Spizzico M, Tallini M (2005) Studio idrochimico multitemporale delle acque sorgive dell'acquifero carsico del Gran Sasso (Italia centrale) per un affinamento del modello idrochimico concettuale. *Giorn Geol Appl* 2:420–428

- Earman S, Campbell AR, Phillips FM, Newman BD (2006) Isotopic exchange between snow and atmospheric water vapor: estimation of the snowmelt component of groundwater recharge in the southwestern United States. *J Geophys Res Atmos*. <https://doi.org/10.1029/2005JD006470>
- Epstein S, Mayeda T (1953) Variation of O18 content of waters from natural sources. *Geochim Cosmochim Acta* 4(5):213–224
- Fazzini M, Bisci C (1999) Clima e neve sul massiccio del Gran Sasso. *Neve e Valanghe* 36
- Ford DC, Williams P (2007) *Karst hydrogeology and geomorphology*. Wiley, Chichester, p 562. <https://doi.org/10.1002/9781118684986>
- Giustini F, Brilli M, Patera A (2016) Mapping oxygen stable isotopes of precipitation in Italy. *J Hydrol Reg Stud* 8:162–181. <https://doi.org/10.1016/j.ejrh.2016.04.001>
- Goldscheider N, Meiman J, Pronk M, Smart C (2008) Tracer tests in karst hydrogeology and speleology. *Int J Speleol* 37(1):27–40
- González-Trinidad J, Pacheco-Guerrero A, Jénez-Ferreira H, Bautista-Capetillo C, Hernández-Antonio A (2017) Identifying groundwater recharge sites through environmental stable isotopes in an alluvial aquifer. *Water* 9(8):569. <https://doi.org/10.3390/w9080569>
- Iacurto S, Grelle G, de Filippi FM, Sappa G (2021) Karst recharge areas identified by combined application of isotopes and hydrogeological Budget. *Water* 13(14):1965–1968. <https://doi.org/10.3390/w13141965>
- Jasechko S, Wassenaar LL, Mayer B (2017) Isotopic evidence for widespread cold-season-biased groundwater recharge and young streamflow across central Canada. *Hydrol Process* 31(12):2196–2209. <https://doi.org/10.1002/hyp.11175>
- Jódar J, Herms I, Lamban LJ, Martos-Rosillo S, Herrera-Lameli C, Urrutia J, Soler A, Custodio E (2021) Isotopic content in high mountain karst aquifers as a proxy for climate change impact in Mediterranean zones: the Port del Comte karst aquifer (SE Pyrenees Catalonia Spain). *Sci Tot Environ* 790:148036. <https://doi.org/10.1016/j.scitotenv.2021.148036>
- Longinelli A, Selmo E (2003) Isotopic composition of precipitation in Italy: a first overall map. *J Hydrol* 270(1–2):75–88. [https://doi.org/10.1016/S0022-1694\(02\)00281-0](https://doi.org/10.1016/S0022-1694(02)00281-0)
- Lorenzi V, Sbarbati C, Banzato F, Lacchini A, Petitta M (2022) Recharge assessment of the Gran Sasso aquifer (Central Italy): time-variable infiltration and influence of snow cover extension. *J Hydrol Reg Stud* 41:101090. <https://doi.org/10.1016/j.ejrh.2022.101090>
- Minissale A, Vaselli O (2011) Karst springs as “natural” pluviometers: Constraints on the isotopic composition of rainfall in the Apennines of central Italy. *Appl Geochem* 26:838–852. <https://doi.org/10.1016/j.apgeochem.2011.02.005>
- Petaccia R, Rusi S (2008) Idrogeologia delle sorgenti del Ruzzo (Gran Sasso d’Italia). *Giornale Geol Appl* 8(1):17–28
- Petitta M, Tallini M (2002) Idrodinamica sotterranea del massiccio del Gran Sasso (Abruzzo): Nuove indagini idrologiche, idrogeologiche e idrochimiche (1994–2001). *Boll Della Soc Geol Ital* 121(3):343–363
- Petitta M, Caschetto M, Galassi DMP, Aravena R (2015) Dual-flow in karst aquifers toward a steady discharge spring (Presciano, Central Italy): influences on a subsurface groundwater dependent ecosystem and on changes related to post-earthquake hydrodynamics. *Environ Earth Sci* 73:2609–2625. <https://doi.org/10.1007/s12665-014-3440-1>
- Petitta M, Mastrorillo L, Preziosi E, Banzato F, Barberio MD, Billi A, Cambi C, De Luca G, Di Carlo G, Di Curzio D, Di Salvo C, Nanni T, Palpacelli S, Risi S, Saroli M, Tallini M, Tazioli A, Valigi D, Vivalda P, Doglioni C (2018) Water-table and discharge changes associated with the 2016–2017 seismic sequence in central Italy: hydrogeological data and a conceptual model for fractured carbonate aquifers. *Hydrogeol J* 26:1009–1026. <https://doi.org/10.1007/s10040-017-1717-7>
- Petitta M, Banzato F, Lorenzi V, Matani E, Sbarbati C (2022) Determining recharge distribution in fractured carbonate aquifers in central Italy using environmental isotopes: snowpack cover as an indicator for future availability of groundwater resources. *Hydrogeol J* 30(5):1619–1636. <https://doi.org/10.1007/s10040-022-02501-9>
- Rusjan S, Sapač K, Petrič M, Lojen S, Bezak N (2019) Identifying the hydrological behavior of a complex karst system using stable isotopes. *J Hydrol* 577:123956. <https://doi.org/10.1016/j.jhydrol.2019.123956>
- Sappa G, Vitale S, Ferranti F (2018) Identifying karst aquifer recharge areas using environmental isotopes: a case study in Central Italy. *Geosciences* 8(9):351. <https://doi.org/10.3390/geosciences8090351>
- Scozzafava M, Tallini M (2001) Net infiltration in the Gran Sasso Massif of central Italy using the Thornthwaite water budget and curve-number method. *Hydrogeol J* 9:461–475. <https://doi.org/10.1007/s100400100151>
- Tallini M, Parisse B, Petitta M, Spizzico M (2013) Long-term spatio-temporal hydrochemical and 222Rn tracing to investigate groundwater flow and water–rock interaction in the Gran Sasso (central Italy) carbonate aquifer. *Hydrogeol J* 21:1447–1467. <https://doi.org/10.1007/s10040-013-1023-y>
- Tallini M, Adinolfi Falcone R, Carucci V, Falgiani A, Parisse B, Petitta M (2014) Isotope hydrology and geochemical modeling: new insights into the recharge processes and water–rock interactions of a fissured carbonate aquifer (Gran Sasso, central Italy). *Environ Earth Sci* 72:4957–4971. <https://doi.org/10.1007/s12665-014-3364-9>
- Taylor CJ, Greene EA (2008) Hydrogeologic characterization and methods used in the investigation of karst hydrology. In: Rosenberry DO, LaBaugh JW (eds) *Field techniques for estimating water fluxes between surface water and ground Water*. US Geological Survey, Reston, pp 71–114
- Vespasiano G, Apollaro C, De Rosa R, Muto F, Larosa S, Fiebig J, Mulch A, Marini L (2015) The small spring method (SSM) for the definition of stable isotope e elevation relationships in Northern Calabria (Southern Italy). *Appl Geochem* 63:333–346. <https://doi.org/10.1016/j.apgeochem.2015.10.001>
- Wachniew P (2015) Environmental tracers as a tool in groundwater vulnerability assessment. *Acque Sotterranee-Italian J Groundwater*. <https://doi.org/10.7343/as-108-15-0135>

**Publisher's Note** Springer Nature remains neutral with regard to jurisdictional claims in published maps and institutional affiliations.